PCCP

PAPER

View Article Online
View Journal

Cite this: DOI: 10.1039/c5cp01286d

Stimulated emission in cryogenic samples doped with free-base tetraazaporphine

Serguei Arabei,[a] John G. McCaffrey,[b] Jean-Pierre Galaup,[c] Niloufar Shafizadeh[d] and Claudine Crépin*[d]

Received 4th March 2015,
Accepted 1st May 2015

DOI: 10.1039/c5cp01286d

www.rsc.org/pccp

Thin cryogenic samples of inert gas solids doped with free-base tetraazaporphine (H_2TAP) were irradiated with a tunable pulsed laser. Under resonant electronic excitation of the guest, specific vibronic transitions of the fluorescence spectra were found to be strongly enhanced with only a moderate increase of the laser power. This enhancement is due to stimulated emission (SE). The characteristics of SE bands are described in the three hosts (Ar, N_2, and Ne) explored, as well as their excitation spectra. SE is observed in transitions involving different vibrational modes of the guest, depending on the host and the electronic excitation. The results are discussed in comparison with previous works on other tetrapyrrolic molecules trapped in inert gas matrices. From this comparison the key features required to observe SE are deduced to be: (1) SE can be obtained with various tetrapyrrolic molecules; (2) free-base molecules are preferable to their metallo-counterparts; (3) the results highlight a specific molecular vibrational mode involved in the process; and (4) cryogenic crystal structures are also of importance in the detection of SE.

I. Introduction

Porphyrins (Ps) and their synthetic analogues, phthalocyanines (Pcs), attract considerable interest because of their constantly expanding use in practical applications such as artificial photosynthesis,[1,2] organic solar cells,[3–6] optical memory elements,[7,8] sensors to monitor the environment,[9,10] medical drugs and antibiotics,[11] and photosensitizers for photodynamic therapy.[12–14] Despite the long history of investigations of these compounds which has provided a substantial body of experimental and theoretical data needed to describe their physical, chemical, photochemical, and spectral properties, as well as significant progress in their synthesis, the attention this class of compounds receives does not abate.[15] Moreover, from a fundamental point of view, an essential stage in the implementation of actual applied problems is the use of spectroscopy in establishing reliable 'structure–property' correlations to identify the detailed mechanisms of relaxation at different levels of molecular organization.

An important characteristic of Ps and Pcs is their large oscillator strengths in the visible spectral region[16–20] and as a consequence, these compounds are frequently used as dye materials.[21,22] Their intense absorption bands, high values of fluorescence quantum yields, thermal and photo-stabilities allow these tetrapyrrolic molecules to be of interest as candidates for lasing devices. Such investigations were conducted in the 1960s and stimulated emission (SE) was first observed in a solution of free-base phthalocyanine[23] (H_2Pc), magnesium phthalocyanine[23] (MgPc) and chloro-aluminium phthalocyanine[24,25] (AlClPc). In these experiments, SE was obtained with pulsed ruby laser excitation and within a resonator cavity of 2.0–2.5 cm length. More recently, we performed luminescence studies on cryogenic matrices doped with Pcs which revealed the occurrence of SE in thin samples, without a resonator cavity.[26] This phenomenon was characterized by a dramatic intensity increase of specific vibronic fluorescence lines of H_2Pc or zinc phthalocynanine (ZnPc) with a moderate increase of the laser pump intensity. These results open up the way for applied research on micron-sized solid-state laser active media based on Pc-doped materials. The first step in such a work is complete characterization of the system and the conditions required to obtain and optimize SE.

The observed dramatic intensity enhancement with a slight increase of the laser pump power was attributed to SE on the basis of (i) the existence of a well-defined threshold in the laser power dependence, (ii) the dependence on the concentration of dopants, (iii) the narrowness of the SE line in comparison with the width of fluorescence bands, and (iv) the shortness of the SE transition lifetime in comparison with that of other emission bands. In fact the SE bands were found to exhibit the same

[a] Belarusian State Agrarian Technical University, Minsk, Belarus
[b] Department of Chemistry, Maynooth University, NUI – Maynooth, County Kildare, Ireland
[c] Laboratoire Aimé Cotton, UMR9188 CNRS – Université Paris-Sud 11, F-91405 Orsay, France
[d] Institut des Sciences Moléculaires d'Orsay, UMR8214 CNRS – Université Paris-Sud 11, F-91405 Orsay, France. E-mail: claudine.crepin-gilbert@u-psud.fr; Tel: +33 1 69 15 75 39

temporal and spectral profiles as the laser pulse.[26] SE was observed in Ne, Ar, Kr and N_2 matrices doped with H_2Pc and ZnPc, but not in Xe matrices. The high fluorescence yield of Pcs is not preserved in solid Xe because of an efficient intersystem crossing from the excited singlet state to the lower lying triplet state due to the external ''heavy'' atom effect.[27] SE corresponds to vibronic transitions between the vibrationless level of the first excited singlet state ($v = 0$) to specific vibrational levels of the ground electronic state. This vibrational level corresponds to the excitation of the same vibrational mode in H_2Pc and ZnPc (vibrational frequencies $\sim$1550 cm^{-1} and 1525 cm^{-1} respectively). We have also explored cryogenic matrices doped with tetrabenzoporphines (TBP).[28,29] TBPs and Pcs are closely related molecules, the most important difference being the replacement of the four bridging nitrogen atoms in Pcs by carbon atoms (see Fig. 1). SE was observed in matrices doped with the free-base TBP (H_2TBP), but not with its zinc counterpart (ZnTBP). In the latter case, the phosphorescence of the molecule was recorded,[28] revealing an efficient intersystem crossing to the triplet state after laser excitation, enhanced by the presence of the internal ''heavy'' metal atom. As in the case of Pc trapped in solid Xe, this non-radiative path stops the SE process. Interestingly, the vibrational modes involved in SE observed with H_2Pc and H_2TBP doped samples are very similar, they correspond to an asymmetric stretch of bridge C–N–C (C–C–C respectively) bonds in the central ring.[30–32]

This paper aims to present an in-depth investigation of the molecular properties of tetrapyrrolic systems, based on free-base tetraazaporphine (H_2TAP), giving rise to SE in cryogenic solids. This goal is achieved by exploring a new system, closely related to the previous ones (H_2Pc and H_2TBP), where SE was observed. Similar to porphine (H_2P), which is the parent molecule of the porphyrins, H_2TAP is, as shown in Fig. 1, the parent molecule of the Pc family. The vibrational structure of these parent molecules is simplified compared to H_2Pc and H_2TBP. We have recently studied the spectroscopy of H_2TAP in Ne, Ar and N_2 matrices[33] to get a clear assignment of the vibronic structure of the absorption, emission and excitation spectra of these systems. The absorption spectra of H_2TAP, and generally of the free-bases of phthalocyanines, are dominated by two fully allowed transitions called $Q_x(S_1–S_0)$ and $Q_y(S_2–S_0)$, situated in H_2TAP at around 600 and 520 nm, respectively, the exact wavelengths depending on the nature of the host. In the free-bases, there are two stable tautomers due to the migration of the two hydrogen atoms between the four nitrogen atoms in the inner cavity (Fig. 1) which give rise to different spectroscopic signatures when isolated in low temperature solids.[34,35] Besides this effect, the molecule can be embedded in various crystallographic sites. Because of the presence of multiple trapping sites for H_2TAP, the spectra are complex. The laser power was kept low for spectroscopic purposes in matrices, but when the laser power increases, SE also appears in these samples. The present study on H_2TAP in cryogenic solids provides new important data on the process of SE. Despite having a very similar chemical structure to H_2Pc, H_2TBP and H_2TAP, differences exist that influence the SE phenomena. For instance, its simplified vibrational structure can be used to highlight the role of vibrational motion in the SE transitions. H_2TAP has a low fluorescence quantum yield[36] compared to H_2Pc and H_2TBP and exhibits strong electron phonon coupling observed in its electronic spectroscopy.[33] These two characteristics could present problems which need to be overcome to detect SE, and could also modify some of the SE properties.

After a brief description of the experimental set-up in Part II, the results related to the observation of SE in H_2TAP-doped matrices are reported in Part III. The discussion in Part IV is focused on the properties of the samples where SE is observed, including the cases of H_2Pc and H_2TBP dopants. This is followed by a short conclusion (Part V).

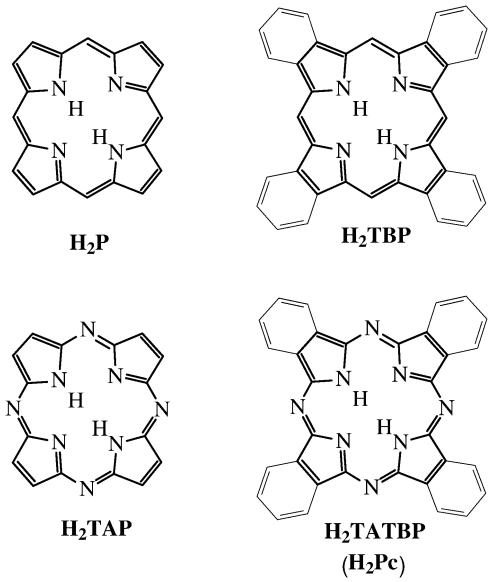

Fig. 1 Schemes of the free-base tetrapyrrolic molecules of interest: porphine [H_2P], tetrabenzoporphine [H_2TBP], tetraazaporphine [H_2TAP] and phthalocyanine (or tetraazatetrabenzoporphine) [H_2Pc or H_2TATBP].

II. Experimental

The experimental set-up is the same as that described in ref. 33 so only the main features are reported here.

H_2TAP powder was synthesized utilizing the method of Makarova *et al.*[37] Samples were obtained by deposition of a gaseous mixture of H_2TAP and host material onto the cold sapphire window of a closed cycle helium cryostat (APD DE 202FF) maintained at 20 K during deposition of Ar and N_2, and at 8 K for deposition of Ne. The mixture was produced by flowing the host gas through a home-built oven, as described in ref. 28, where the H_2TAP powder is heated to about 190 °C. The host gas carries the H_2TAP vapor to the cold window where both are co-deposited. The visible absorption spectrum of the sample around the origin of the $S_1–S_0$ transition was monitored during deposition in order to check the quality of the sample in terms of good isolation of monomers and to reach the large optical density (OD $\sim$ 1) required to produce SE. After deposition, the working temperature was set to 8 K for all samples.

Absorption, emission and excitation spectra were recorded using a 0.6 m Jobin-Yvon monochromator equipped with an iCCD camera (Andor DH720) as the detector. The spectral resolution was of few cm^{-1}. A tungsten lamp was used as the light source for absorption spectra. Emission, and especially stimulated emission, was produced with tuneable dye laser excitation using one or the other of the two lasers as detailed in ref. 33. They covered the spectral range of 500–610 nm corresponding to the two first electronic transitions towards $S_1(Q_x)$ and $S_2(Q_y)$ states of H_2TAP. The laser line width was less than 1 cm^{-1}, so that the resolution of excitation spectra obtained by scanning the laser frequency was better than that of emission spectra. Some experiments on H_2TAP/Ar samples were also performed using an OPO laser (Continuum Horizon) covering all the visible spectral range with a linewidth of $\sim$5 cm^{-1}. The use of the iCCD camera when scanning the laser frequency resulted in the measurement of 2D-excitation–emission (EEM) spectra, which are very useful for a direct comparison between fluorescence and SE bands. The laser intensity was varied between 1 and 30 mW, and the laser beam was slightly focused to reach a spot of $\sim$3 mm diameter on the sample.

III. Results

The fluorescence spectra of H_2TAP trapped in Ne, Ar and N_2 have been recorded with laser excitation in the S_1 and S_2 electronic states.[33] The spectra exhibit a vibronic structure corresponding to the emission from the vibrationless level of S_1 to various vibrational levels of the ground state, up to an energy of around 1600 cm^{-1}. In most cases, each vibronic band is broad and structured due to the emission from different trapping sites (see Fig. 4 and 5 of ref. 33). This is due to a strong electron–phonon coupling in the S_1–S_0 transition which prevents the excitation of a unique well-defined trapping site (or family of sites) whatever the excitation laser energy is. Nevertheless, when the excitation laser power increases, we have been able to observe few narrow and intense emission lines at specific wavelengths superposed on the fluorescence bands. These lines have the characteristics of stimulated emission (SE), as previously described in the case of H_2Pc isolated in inert gas matrices.[26] This effect appears in the three hosts studied. A complete description of the phenomenon observed in Ar matrices is provided, followed by a less detailed report in N_2 and Ne matrices.

III.1. H_2TAP/Ar

Fig. 2 shows the part of the emission spectrum where the SE bands are observed in H_2TAP/Ar samples. The laser wavelength (604.8 nm) is tuned to the maximum of the 0–0 S_1–S_0 absorption band. Three structured vibronic bands are clearly observed with a low laser power (blue curve). In each band, the line of highest frequency corresponds to the emission from the directly excited family of sites, whereas the other structures correspond to the emission from other trapping sites with less energetic S_1–S_0 transitions.† Emission in the

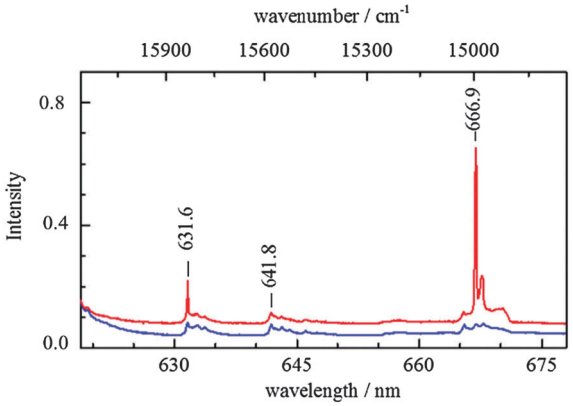

Fig. 2 Fluorescence spectra and stimulated emission in H_2TAP/Ar samples at 8 K with a laser excitation at 604.8 nm (dye laser); laser power: 1 mW (blue) and 10 mW (red).

665–670 nm range exhibits a even more complex structure because of the overlap between two vibronic bands, corresponding to vibrational modes of the ground state at 1506 cm^{-1} and 1540 cm^{-1}.[33] With a higher laser power, narrow SE bands appear (red curve). A relatively weak peak is observed at 631.6 nm, corresponding to the emission from the main trapping site to $v = 1$ of the mode at 700 cm^{-1}. The most intense SE band at 666.9 nm (red line) is observed in the middle of the complex vibronic structure, so that it is not clear if the transition involves the mode at 1540 cm^{-1} of the main site or the mode at 1506 cm^{-1} of a secondary site. Similarly, the origin of the weaker SE line in the red side of the maximum (667.8 nm) cannot be deduced only from this spectrum. In fact, SE bands appear at slightly different wavelengths in the 665–668 nm spectral range depending on the excitation energy inside the 0–0 S_1–S_0 absorption band. The full data can be extracted from 2D EEM spectra, such as that presented in Fig. 3a.

SE bands appear as vertical lines in the 2D EEM spectrum (Fig. 3a), highlighting the relative independence of their wavelengths on the excitation energy. The excitation spectrum of the intense SE band at 666.9 nm (Fig. 3c, red curve) shows a narrow band centered at 604.8 nm and broad features in its blue side, corresponding to the excitation of phonons. Taking 604.8 nm as the electronic origin of the sites responsible for this SE band, we conclude that the stimulated emission occurs toward the vibrational excitation of the mode at 1540 cm^{-1}. All the vertical lines of lower emission energy present a more or less defined band of lowest energy in excitation, which can be considered as electronic origins; these origins are aligned in the 2D EEM spectrum (yellow dotted line in Fig. 3a). All these SE bands involve the same vibrational level of the ground state, *i.e.* the mode at 1540 cm^{-1}. However, a peak appears in the 2D EEM out of the range of the previously described behavior, whose related emission and excitation spectra are depicted in blue in Fig. 3b and c. Both spectra show single and specifically narrow bands (line widths $\sim$3–4 cm^{-1}), one at 604.9 nm in excitation and a new one at 665.5 nm in emission, meaning that in this case, SE appears in a vibronic transition involving the mode at 1506 cm^{-1}. One can notice that the latter SE band appears at a

† We call "family of sites" one or more trapping sites where the molecules have the same S_1–S_0 transition energy; for sake of simplicity, the term "site" will be used as "family of sites" hereafter.

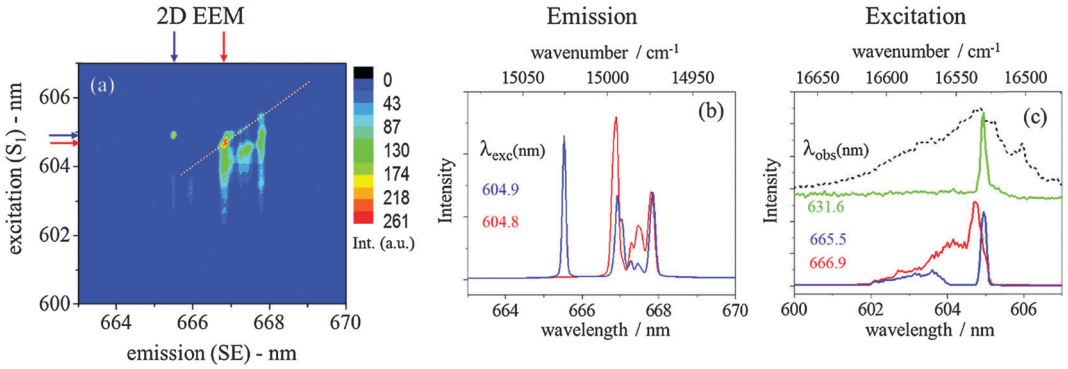

Fig. 3 H_2TAP/Ar samples at 8 K: (a) 2D EEM spectrum, excitation in the spectral range of the S_1 origin band, emission in the spectral range of multiple SE bands, laser power (OPO laser): 15 mW; the yellow dotted line follows the origins of excitation spectra taken at several emission wavelengths (vertical features, see text). Emission (b) and excitation (c) spectra are shown for particular values of excitation and detected wavelengths, respectively, reported in (a) as small blue and red arrows; these spectra are obtained by horizontal and vertical cuts, respectively, of the 2D EEM spectrum at the specified wavelengths; colors of arrows in (a) correspond to colors of the curves in (b) and (c); in the upper part of (c), the excitation spectrum of the band at 631.6 nm (green line) and the absorption spectrum (black dots) are reported for comparison.

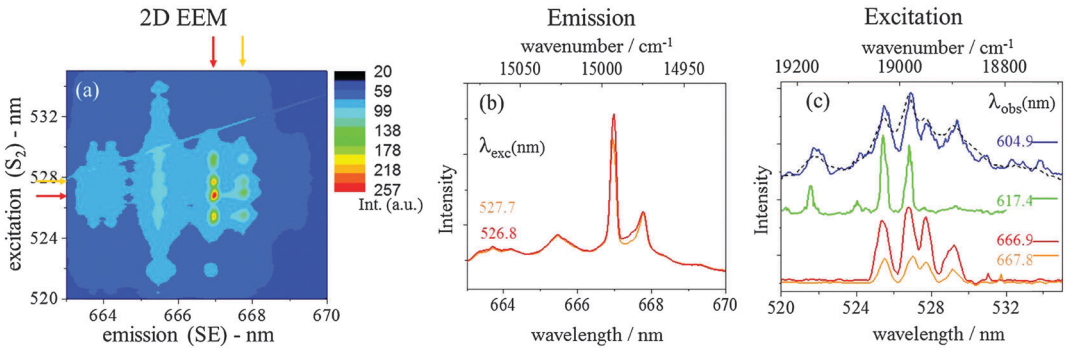

Fig. 4 H_2TAP/Ar samples at 8 K: (a) 2D EEM spectrum, excitation in the spectral range of the S_2 origin band, emission in the spectral range of multiple SE bands, laser power (dye laser): 12 mW; the diagonal line is due to a ghost and follows the excitation wavelength. (b) Emission spectra extracted from horizontal cuts (horizontal arrows in (a)) of the 2D EEM spectrum at 526.8 nm (red) and at 527.7 nm (orange). (c) Excitation spectra extracted from vertical cuts (vertical arrows in (a)) of the 2D EEM spectrum at 666.9 nm (red) and at 667.8 nm (orange); in these excitation spectra, the SE band intensity is divided by the fluorescence intensity to be emphasized; are reported for comparison the fluorescence excitation spectrum recorded at 604.9 nm (blue curve), the absorption profile (black dots) and the excitation spectrum recorded at 617.4 nm, a weak SE band involving the mode at 335 cm^{-1} (green curve).

high irradiation energy, in an excitation wavelength range of 0.1 nm, explaining why it is absent in the example of Fig. 2 and in the red spectrum of Fig. 3b. Its different behavior can also be seen in the shapes of the excitation spectra (Fig. 3c).

No SE band in the 665–668 nm spectral range was detected when exciting a vibrational level of the S_1 state under our experimental conditions, except that SE at 665.5 nm was observed in one sample when exciting at 598.6 nm, corresponding to the excitation of the vibrational mode at 175 cm^{-1} above the excited state. Being a nonlinear effect, the intensity of SE bands (and their appearance) can, in contrast to their frequencies, vary considerably when the experimental conditions are only slightly modified. Besides, these intense SE bands were easily detected when exciting the S_2 state. Fig. 4 reports the corresponding 2D EEM spectrum (panel a), together with the emission (panel b) and excitation (panel c) spectra extracted from it. SE is along the same verticals as in Fig. 3a (same emission frequencies), but appears also in horizontal lines: all the detected SE bands have very similar excitation spectra (Fig. 4c). The spectral range around the origin of the S_2 state is complex because of couplings between the $v = 0$ level of the S_2 state and various vibrationally excited levels of the S_1 state.[38] Excitation bands are broad ($\sim$30 cm^{-1}), similar to that of fluorescence excitation (blue curve in Fig. 4c), and only slightly narrower than absorption bands (dots in Fig. 4c). There is a complete lack of site selectivity when exciting in the S_2 state, as previously mentioned in the fluorescence study.[33] Moreover, only SE bands with $\lambda_{SE} \geq 666.9$ nm were clearly detected and these bands have broader excitation spectra in the spectral range of the S_1 origin (Fig. 3). SE at 665.5 nm was detected at its threshold when exciting in the S_2 state, so that its excitation spectrum was difficult to extract. It seems that the S_2 excitation bands are slightly red shifted in this specific case ($\sim$18 cm^{-1}) from the bands shown in Fig. 4c.

When exciting in the S_2 state (between 520 and 530 nm), two weak SE bands are detected at 617.4 nm and 617.8 nm. Their frequencies are red shifted by $\sim$335 cm^{-1} from the peaks at 604.8 and 605.2 nm of the absorption band of the S_1 origin, and

thus are assigned to emission toward the vibrational level at 335 cm^{-1} of the ground state. They cannot be detected when exciting the S_1 origin because of the scattering light of the laser when tuned in this range. The excitation spectrum of the 617.4 nm band, reported in Fig. 4c (green curve), exhibits slightly narrower bands than that of the SE in the 666–668 nm range. That of the 617.8 nm band shows slightly broader bands redshifted by $\sim$10 cm^{-1}, *i.e.* the same shift as between the two weak SE bands. It seems that these SE bands appear in a more restrictive selection of sites, allowing a slight selectivity in the S_2 state. In addition, the threshold effect reduces the number of excitation bands for this weak SE.

The weak SE band at 631.6 nm (Fig. 2) was not detected with the S_2 excitation. Its excitation spectra in the S_1 origin overlaps that of the SE band at 665.5 nm. Both show a narrow excitation band corresponding to the same well defined trapping site (Fig. 3c). With an increase in the laser power when tuned at 604.9 nm, another weak SE band at 641.8 nm was detected. This new SE has the same excitation spectrum as the band at 631.6 nm which includes two bands in the first vibrational levels of the S_1 states, at 598.7 nm and 593.1 nm. All these bands are very sharp. The SE spectroscopy of this specific trapping site gives rise to precise measurements of vibrational levels: at 174 $\pm$ 2 cm^{-1} and 330 $\pm$ 1 cm^{-1} in the S_1 state, at 700 $\pm$ 1, 951 $\pm$ 1 and 1505 $\pm$ 1 cm^{-1} in the ground state. SE bands at 617.4 nm and 617.8 nm are most probably coming from two tautomers embedded in the same trapping site, as was observed in the case of H_2TBP/Ar samples where similar spectral shifts were observed in the S_1 and S_2 excitation of tautomers,[28] suggesting that they come from another site than the previously discussed one, which cannot be associated with SE doublets. This SE doublet corresponds to an emission toward the vibrational level at 335 $\pm$ 1 cm^{-1} in the ground state.

In summary, SE in H_2TAP/Ar samples is rich and site dependent. In the specific site corresponding to the maximum absorption, SE is detected in several vibronic bands, which are the most intense bands in the fluorescence spectrum.[33] SE coming from other sites is detected on another vibronic transition, involving only the mode at 1540 cm^{-1}, and seems to be more intense. The latter SE was the unique one easily observed when exciting the S_2 state. Most of the SE bands are detected at the same wavelengths under excitation in more than one energy range, corresponding to different electronic and/or vibronic excited levels. This behavior, added to the characteristics depicted in the Introduction, prevents to assign the so-called SE bands to resonance Raman bands. We haven't verified systematically the occurrence of all the SE characteristics for all the observed SE bands, but the similarities in the behaviors upon laser energies and frequencies, upon samples, between all these specific emission bands allow to assign all of them to SE coming from the amplification of spontaneous emission.

III.2. H_2TAP/N_2

In nitrogen matrices, SE is only observed in the 664–666 nm spectral range. Three clear SE bands appear, at 664.2, 665.1 and 665.6 nm, when exciting the origins of the S_1 and/or S_2 states, as shown in Fig. 5a. In the S_1 state, SE is induced by excitation in broad phonon bands, as revealed by the long intense vertical segments in the 2D EEM spectrum evident in Fig. 5b, on the blue side of the maximum of absorption at around 603.3 nm. The excitation in the S_2 state is more structured (Fig. 5c and d), but, because of the complexity of S_2–S_1 vibronic coupling in this spectral range, its structure cannot be used to assign correctly the SE bands. However, the band at 664.2 nm is at the exact wavelength of the maximum fluorescence in this spectral range (Fig. 5a): from the fluorescence analysis of ref. 33, it corresponds to the transition towards the vibrational excitation of the mode at 1505 cm^{-1} in the site of lower energy in absorption (603.8 nm). The energy of the second band at 665.1 nm matches with the vibronic transition involving the mode at 1538 cm^{-1} for the main absorption site at 603.3 nm. Following this assignment, the third band is thus assigned to the same vibronic transition occurring in sites having a less energetic S_1–S_0 transition ($\lambda > 603.3$ nm).

The previous assignment was confirmed thanks to a very weak SE signal detected when exciting the most intense vibronic transition in the S_1 excited state for the two main SE bands (Fig. 6): the excitation peak of the most energetic SE at 664.2 nm (553.8 nm) is red shifted from that of SE at 665.1 nm (553.4 nm), proving that both SE do not involve the same vibrational mode in the ground state. The shift between the two peaks (13 cm^{-1}) reflects the shift in the S_1–S_0 absorption origins of the two distinct excited sites. The shift between the two SE bands (20 cm^{-1}) reflects the combination of distinct sites and distinct vibrational modes (1538–1505 = 13 + 20). This simple arithmetic allows us to assign the vibrational level excited in the S_1 state to a mode frequency of 1496 cm^{-1}. This mode corresponds to the most intense vibronic band of the S_1–S_0 transition in the excitation spectra.[33]

For nitrogen, in contrast to argon, the excitation spectra in the region of the S_2 origin depend on the detected SE (Fig. 5d). In all spectra, the structures are broad (20 to 50 cm^{-1}), preventing any precise assignment. One can remark that the simplest structure is obtained when monitoring the lower energy SE (λ_{obs} = 665.6 nm), giving a better defined shift between the S_1 and S_2 state ($\sim$2370 cm^{-1}) in the corresponding site than in the other cases.

III.3. H_2TAP/Ne

SE in Ne is difficult to detect under our experimental conditions. With our cryostat limited to a minimum temperature of 8 K, the deposited samples are soft and delicate. As SE requires relatively a high laser power and strong absorption, it is very easy to create holes in the samples when looking for the SE phenomenon. Nevertheless, we detected SE in the 660–662 nm spectral range when exciting in the S_2 state. Fig. 7 shows the SE doublet, compared to fluorescence in the same spectral range. In Ne, absorption and fluorescence spectra show well resolved doublets assigned to the two NH tautomers occupying the same main trapping site.[33] In the 660–662 nm spectral range, there are two doublets corresponding to the two vibronic transitions involving the vibrational

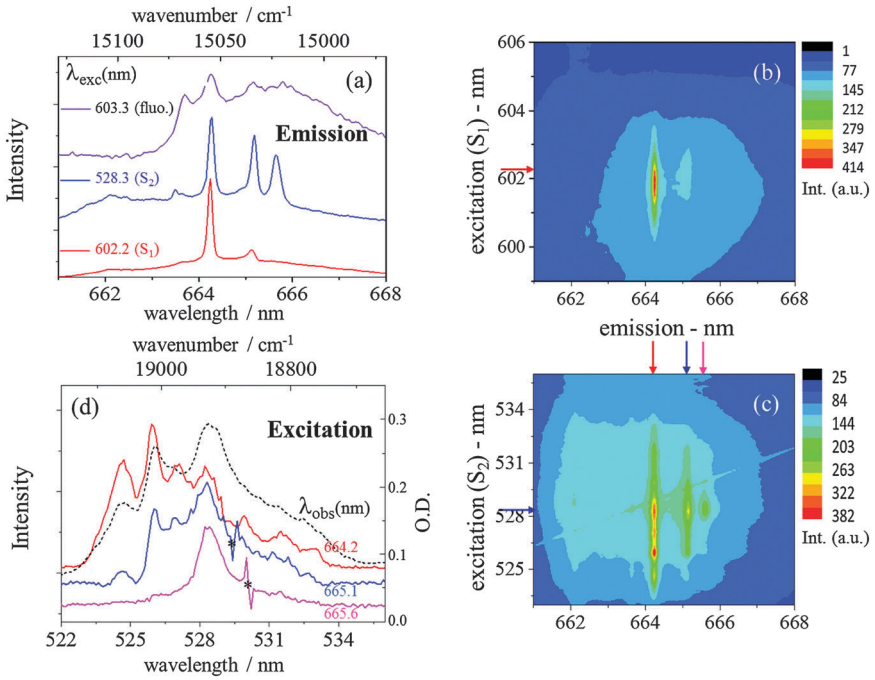

Fig. 5 H_2TAP/N_2 samples at 8 K: (a) SE bands detected when exciting the S_1 and S_2 states (red and blue lines, respectively); the fluorescence spectrum obtained when exciting in the maximum absorption is reported as violet line for comparison. (b) 2D EEM spectrum, excitation in the spectral range of the S_1 origin band, and emission in the spectral range of multiple SE bands, laser power (dye laser): 8 mW. (c) 2D EEM spectrum, excitation in the spectral range of the S_2 origin band, and emission in the spectral range of multiple SE bands, laser power (dye laser): 12 mW; the diagonal line is due to a ghost and follows the excitation wavelength. (d) Excitation spectra of SE at 664.2 nm (red), 665.1 nm (blue), and 665.6 nm (magenta); the absorption spectrum in black dots; these spectra are obtained by dividing the SE signal by the fluorescence signal detected in the wing of the vibronic band to emphasize the non linear SE signal; features induced by the ghost are marked with *. Colored arrows in the 2D EEM spectra correspond to $\lambda_{exc}/\lambda_{obs}$ of spectra in panels (a) and (d) in the same color.

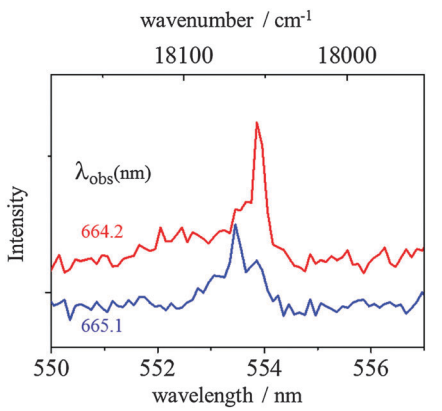

Fig. 6 H_2TAP/N_2 samples at 8 K: excitation spectra of SE at 664.2 nm (red) and 665.1 nm (blue) in the vibrational excited levels of S_1 – laser power (dye laser): 12 mW – these spectra are obtained by dividing the SE signal by the fluorescence signal detected in the wing of the vibronic band to emphasize the non linear SE signal.

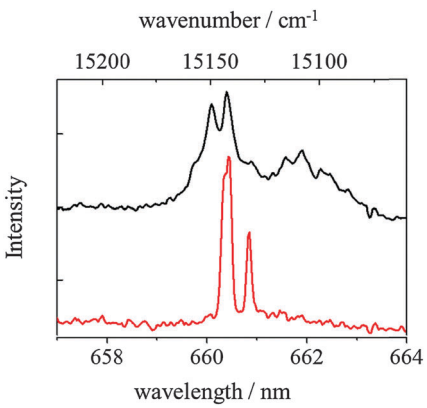

Fig. 7 H_2TAP/Ne samples at 8 K: SE spectrum at λ_{exc} = 524.7 nm (red curve) and fluorescence spectrum at λ_{exc} = 589 nm (black curve).

modes at 1510 and 1544 cm^{-1}. The SE doublet does not correspond to one of the fluorescence doublet (Fig. 7): the most intense SE occurs on the vibronic transition to the mode at 1510 cm^{-1} of the red site, and the other, at lower energy, on the same vibronic transition of a less energetic minor site. As in the case of Ar and N_2 hosts, SE appears in the sites of low energy. The most intense SE band appears broader than the others in Fig. 7, but it shows also a structure: in fact it contains two very close and narrow SE lines coming from two very similar but different sites which cannot be distinguished in absorption and/or fluorescence spectra.

The excitation energy (λ_{exc} = 524.7 nm) is that of one of the most intense bands in the fluorescence excitation spectrum. In spite of several attempts, no excitation spectrum has been recorded, but it seems that SE was obtained only at this wavelength.

IV. Discussion

Stimulated emission was easily observed in cryogenic samples doped with tetrapyrrolic molecules. Whereas its detection is strongly dependent on experimental conditions, especially because of its threshold effect, many characteristics can be established.

In our samples, SE is stimulated by photons coming from the fluorescence of the guest molecule, it is an amplified spontaneous emission. To get SE to occur, the population inversion density (N) between the upper and lower levels involved in the transition must be larger than a threshold value (N_{th}). This value can be evaluated in a simplified model using eqn (1):[39,40]

$$N_{th} = 8\pi n^2 \tau \Delta\nu / \phi \lambda^2 L \quad (1)$$

where n is the refractive index of the solid, τ the excited state lifetime, $\Delta\nu$ the fluorescence line width, ϕ and λ are the fluorescence yield and wavelength of the transition, respectively, and L the length of the photon path through the sample.

It looks surprising that such an amplification of fluorescence by stimulated emission could be reported in thin slabs, 100–200 μm thick typically. We noticed that no SE was observed when using a focused irradiation on a spot with about 100 μm diameter. In contrast, SE was recorded when a few mm spot irradiated the sample, therefore increasing the travel path of light (L), transversally, through the active medium, to a larger value than the sample thickness. We should also be able to increase still the observed SE by improving the collection of the generated light.

Besides these optical considerations, we will discuss the intrinsic properties of the solid systems at play.

IV.1. Molecular properties

Before the laser pulse, none of the vibrational levels of the ground state are populated at cryogenic temperatures. Once v = 0 of the S_1 state is populated after the laser excitation, the population inversion is the same for all the vibronic transitions observed in fluorescence. Eqn (1) shows that SE occurs more easily on transitions of low energy (long wavelength λ) and well observed in fluorescence (high ϕ) when the threshold is smallest.

In all the three molecules H_2Pc, H_2TBP and H_2TAP, there are relatively intense fluorescence bands in the lowest energy part of the vibronic progression, and effectively, the most intense SE bands are detected on these transitions, related to vibrational energies $E_v \sim 1500$–1600 cm^{-1}. Another group of quite intense fluorescence bands involve vibrational levels with $E_v \sim 600$–700 cm^{-1}. SE was detected, weakly, with E_v = 700 cm^{-1} in H_2TAP/Ar samples, and with E_v = 687 cm^{-1} and 730 cm^{-1} in H_2Pc/N_2 samples.[26] The SE bands detected at 617.4 nm and 617.8 nm in H_2TAP doped argon matrices correspond also to a well observed vibronic transition in the fluorescence spectrum ($\sim$335 cm^{-1}), underlining the importance of the ϕ parameter. In H_2Pc and H_2TBP, only one transition has E_v in the specific range: E_v = 1550 cm^{-1} and E_v = 1615 cm^{-1}, respectively.[29,41] Both vibrational modes correspond to the same molecular motions, depicted in Fig. 8 for H_2Pc, and to very active modes in Raman spectroscopy (I = 18 943 and 7234 Å^4 amu^{-1}, respectively, from DFT B3LYP/6-311++G(2d,2p) calculations[42]). The same mode is involved in the SE bands observed in ZnPc trapped in inert gas matrices,[26] and also in the former SE behavior observed in MgPc and AlClPc in solution.[23–25] It should be mentioned that we also performed a few experiments with AlClPc in Ar and N_2 matrices. Weak SE was detected in Ar on the same vibronic transition as that originally observed in the solution-phase experiments.

H_2TAP is thus an interesting case with two modes (Fig. 8) in this energy range: E_v = 1508 cm^{-1} (mode α) and 1549 cm^{-1} (mode β), from DFT calculations[33] (scaled values). Obviously, the mode with molecular motions close to those of the SE mode in H_2Pc is the latter one. On the other hand, the fluorescence intensity of the former one is the highest, as is its Raman activity (1478 and 943 Å^4 amu^{-1} are obtained in DFT B3LYP/6-311++G(2d,2p) calculations for modes α and β, respectively[42]).

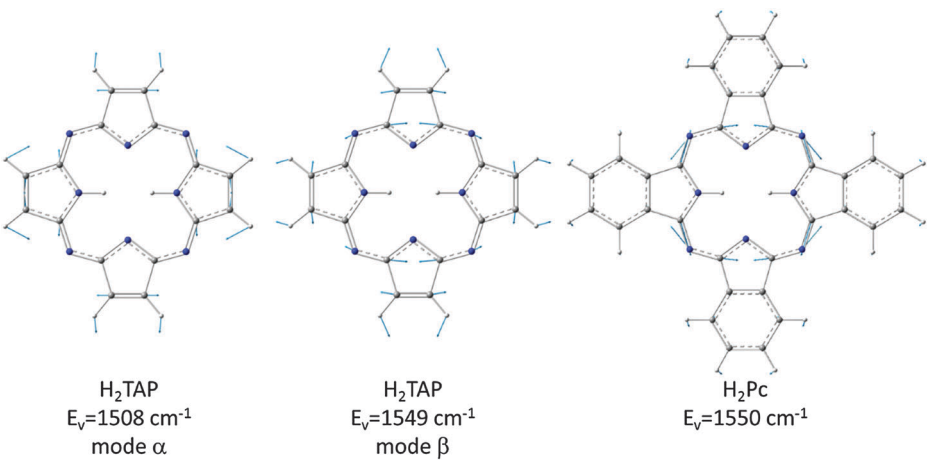

Fig. 8 Vector displacement representation of the vibrations of H_2TAP and H_2Pc exhibiting SE. The vibrational frequencies provided are scaled values from the DFT calculations presented in ref. 31 and 33.

SE is detected on both modes, depending on the host and the trapping site. In Ne, in contrast to Ar and N_2, the fluorescence intensity related to mode α is clearly higher than the other; SE is observed only on the related transition. With similar intensities (ϕ) and wavelengths (λ) on both transitions in Ar and N_2, the site dependence of the SE behavior could come from the vibrational dynamics in the ground state, with a particularly fast vibrational relaxation of mode β, keeping the population inversion at a high level for the 5 ns duration of the laser pulse. Mode specific dynamics may also explain the peculiar SE intensity on that mode for all the explored tetrapyrrolic systems. Nevertheless, one can remark that SE on mode α or β appears when the corresponding fluorescence intensity shows a subtle maximum (*cf.* the blue curve in Fig. 2 for Ar and the violet curve in Fig. 5a for N_2, see below).

The molecules H_2Pc,[16] H_2TBP[19] and H_2TAP[17,18] all have large molar extinction coefficients ε on their Q_x-band (S_1–S_0): with $\log\varepsilon$ values of ~5.2, 4.7 and 4.7 in solution respectively. In all three cases, the $S_1 \rightarrow S_0$ fluorescence is dominated by the 0–0 transition. The main vibronic transition where SE is observed takes only few % of the fluorescence intensity. With a high fluorescence yield, this small ratio is enough to get SE. The fluorescence yields (ϕ_F) measured in different solvents at room temperature showed that $\phi_F(H_2Pc)$ is effectively high (0.7)[43] and that $\phi_F(H_2Pc) > \phi_F(H_2TBP) \gg \phi_F(H_2TAP)$. $\phi_F(H_2TBP)$ is reduced (0.4) because of a larger intersystem crossing quantum yield in H_2TBP than in H_2Pc.[43] Only a value of $\phi_F = 0.17$ was measured for H_2TAP[44] explained by a surprising high quantum yield of internal conversion in this molecule. Whereas all these measurements cannot be strictly compared, the same trend was observed at 77 K with different solvents.[36,45–47] These results cannot be directly applied to our experiments in cryogenic matrices, but we observed that the S_1 lifetime in Ar matrices was reduced from 13 ns for H_2Pc[41] to 4 ns for H_2TAP[33] and that it was effectively difficult to obtain SE with H_2TAP in matrices.

The three molecules are free-bases where NH tautomerisation occurs under electronic excitation.[29,33,35] Solovyov *et al.*[48] obtained a comparison of the efficiency of this process in the three molecules of interest in solution at 77 K: tautomerisation is faster with H_2TBP than with H_2TAP and is slowest with H_2Pc. In our experiments, this effect would reduce the number of absorbers under a prolonged irradiation at a fixed wavelength in resonance with the absorption band of a specific tautomer. Nevertheless, no significant decrease of the main SE emission was observed after such irradiations of tens of minutes in Ar or N_2. On the contrary, in Ne, the SE bands are difficult to observe, as mentioned previously in the case of H_2TAP and in ref. 26. In particular, they disappear after few seconds of irradiation at a constant wavelength: it could be a consequence of the tautomerisation when N is close to N_{th}. The use of metalloporphines or metallophthalocyanines could prevent from the effects of the NH tautomerisation. Unfortunately, the fluorescence yield is reduced in these compounds because of the heavy atom effect, making the detection of SE more difficult. As we have been able to observe SE with ZnPc and not with ZnTBP, it seems, once again, that phthalocyanine is the most convenient case to produce SE.

Under our experimental conditions, it was not possible to quantify more properly the SE efficiency from one molecule to another. However, our results show that with the selection of different tetrapyrrolic molecules, one can obtain SE in a wide spectral range: 660–670 nm with H_2TAP, 720–730 nm with H_2TBP, and 750–760 nm with H_2Pc.

IV.2. Medium properties

The tetrapyrroles of interest (Fig. 1) are large, planar molecules which take the place of several host atoms or nitrogen molecules and may be embedded in different crystallographic planes of the lattice. The trapping sites of H_2P have been simulated in rare gas matrices, giving an idea of the various occupied sites, depending on the host.[49] The main trapping sites are responsible for the band structure observed in absorption and in emission. The structure observed in absorption is very reproducible from one sample to another for the same guest–host mixture. Thus preferential sites definitively exist in each host. Besides this structure and the main trapping sites, a kind of continuum of secondary sites may appear. When this continuum is intense, SE may occur with the same probability in various sites: it is detected in the 2D EEM spectra as a diagonal line of maxima, as was clearly observed in H_2Pc/Ne.[26] Small parts of diagonals can appear in the case of very close sites, giving rise to SE. This is observed, for example, in Fig. 3a (H_2TAP/Ar) for the sites with SE in the 666–668 nm range. SE is thus a tool capable of characterizing the trapping sites.

Absorption and emission bands are usually inhomogeneously broadened because of the diversity of trapping sites, but an additional broadening comes from the electron–phonon coupling in the S_1–S_0 electronic transition, giving rise to blue phonon wings in absorption and red phonon wings in emission. As mentioned previously, fluorescence bands of H_2TAP trapped in Ne, and especially in Ar and N_2, are broad and exhibit large red phonon wings because of a strong electron–phonon coupling. This phonon wing in emission seems to enhance the fluorescence of the less energetic sites (“red sites”), as reported in Fig. 9 in the case of the 0–0 emission band of H_2TAP in Ar where this fluorescence band (in red) is compared with the absorption band of the same transition (black dots). It also shows the absence of emission in the blue part of absorption, which is mainly due to phonons. Only emission from the less energetic sites (energy lower or equal to the maximum of 0–0 absorption band) is clearly observed in the fluorescence spectra, whatever the matrix host and the excitation wavelength is.[33] The photons coming from the 0–0 emission of “blue sites” can be reabsorbed by lower energetic sites, *via* their blue phonon wing in absorption, enhancing the fluorescence from the latter sites and producing a similar spectral effect as the red phonon wings. SE can only be obtained in these “red sites”, as observed. We were able to detect SE in “blue sites” in H_2Pc/N_2 samples[26] where the electron–phonon coupling was weaker. However, the excitation spectra of the different SE bands showed generally large phonon wings. In contrast, in H_2TBP/Ar samples, two SE peaks were observed at very close frequencies

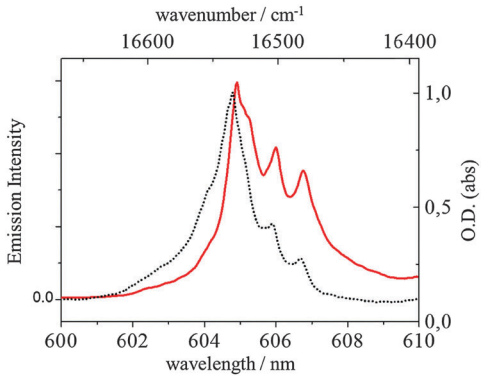

Fig. 9 Fluorescence in the spectral range of the S_1–S_0 origin when exciting the S_2 state (λ_{exc} = 527.0 nm) of H_2TAP trapped in Ar (red curve) compared to the absorption spectrum of the same sample (black dots).

(separated by 4 cm^{-1}) with clearly separated excitation spectra:[28] SE cannot be induced in a site when exciting the other despite their very close transition energies. SE highlights that the electron–phonon coupling effects have a pronounced site specificity.

With H_2TAP, the red wing of fluorescence bands is composed of the emission from less energetic sites than the site directly excited and by phonon wings. This has another consequence: the red wing of the band on mode α artificially enhances the fluorescence band on mode β. Moreover, photons from this wing can have the same energy as photons of the vibronic transition to mode β, with the effect that they can induce SE on the latter transition. This effect may explain the site dependence observed in Ar and N_2 where these wings are much more important than in Ne. In N_2, the red wings are especially strong, enhancing the fluorescence of the minor site of low energy (603.8 nm): the fluorescence from this site appears always as the most intense, whatever the site directly excited.[33] As expected, the fluorescence of the site at 603.8 nm presents a band more intense on mode α than on mode β (Fig. 5), and SE appears on mode α (664.2 nm). In contrast, when exciting in the maximum absorption (603.3 nm), the fluorescence intensity is larger at the energy of the band associated with mode β than that associated with mode α, because of the fluorescence on mode α of the red sites, inducing SE on mode β (665.1 nm). In Ar, the site where SE is detected on mode α corresponds to the maximum of absorption and also to narrowest fluorescence bands among the various site specific bands ($\Delta\nu \sim 10$ cm^{-1}). This induces a decrease in the threshold (eqn (1)) for all the vibronic transitions, allowing the observation of SE on various transitions, and avoids a large overlap between the bands related to mode α and mode β, giving rise to SE on mode α and not on mode β. However, the differences in intensity previously discussed are so subtle that it is difficult to conclude that it is the only reason of the site dependence of the SE bands in Ar and N_2.

One can notice (Fig. 3c) that the related excitation spectrum in the S_1 state of the site with SE on mode α in Ar does not exhibit a strong phonon band. Similarly, the H_2Pc site in N_2 for which SE in various vibronic bands was observed did not show large phonon bands in the S_1 excitation.[26] A weak electron–phonon coupling makes SE easier, especially because of a narrowing of the fluorescence linewidth ($\Delta\nu$). The linewidth effect is also clearly manifested in the temperature dependence exhibited. When the temperature is raised, $\Delta\nu$ increases by means of coupling with phonons, and the SE efficiency strongly decreases. The pronounced effect this has on the SE is shown in Fig. 10 in comparison with the fluorescence of a H_2Pc/N_2 sample.

IV.3. Spectroscopic remarks

The SE bands are very narrow – at the limit of our experimental resolution – and provide precise spectroscopic data. They can be used to distinguish sites which are spectrally very close, as in the case of the structured SE line observed in H_2TAP/Ne samples (Fig. 7). SE excitation spectra also provide precise spectroscopic data. However, as shown in the Results section, these accurate data concern a limited number of vibronic transitions. In particular, intense absorption occurs mainly in the origins of S_1 and S_2 states and vibrational excitation of the S_1 state does not induce SE usually. Moreover, fluorescence excitation spectra in the S_1 state may also provide well resolved bands, thanks to the fluorescence line narrowing, as observed in our previous matrix studies with tetrapyrrolic molecules.[33,41]

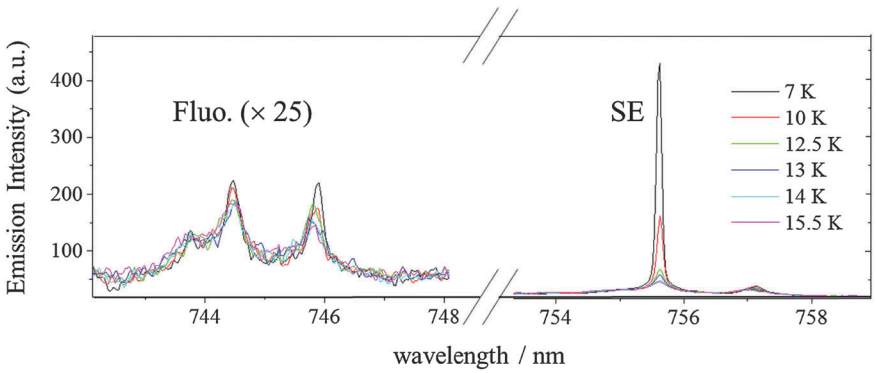

Fig. 10 SE (right) and fluorescence (left) bands obtained with λ_{exc} = 634 nm (S_2) in an H_2Pc/N_2 sample at different temperatures. The two main bands observed in the two spectra correspond to vibronic transitions of two distinct sites. The shoulder detected at 743.7 nm is the signature of a third site. SE occurs only in one site.

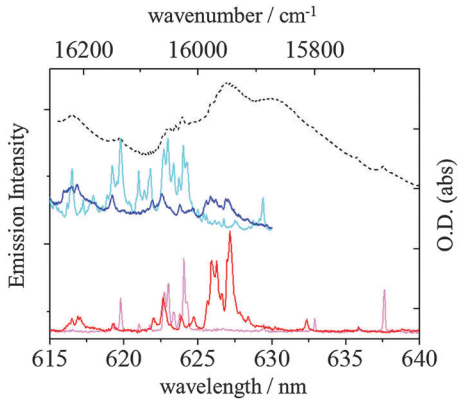

Fig. 11 Excitation spectra in H_2Pc/Ne samples: SE excitation spectra (red and magenta) compared to fluorescence excitation spectra (blue and cyan) around the origin of the S_2 state recorded when probing two sites; absorption in black dashes for comparison. In these samples, there is a well-defined "blue site" for which the improvement between the SE excitation spectrum in magenta (λ_{obs} = 742.6 nm) and the fluorescence excitation spectrum in cyan (λ_{obs} = 666.2 nm) is negligible and a broad continuum of "red sites";[41] the solid blue and red curves present the results corresponding of the maximum of this continuum observed at 669.5 nm in the S_1–S_0 absorption (λ_{obs} = 746.8 nm for SE, in red, and λ_{obs} = 669.5 nm for fluorescence, in blue); the improvement in the spectral resolution is well observed in the latter case.‡

Nevertheless, the present study of H_2TAP/N_2 demonstrates the additional improvement obtained with SE. Because of the large electron–phonon coupling, the two intense vibronic bands corresponding to vibrational energy of $\sim$1500 cm^{-1} in the S_1 excited state were not resolved in the fluorescence excitation spectrum.[33] In contrast, the SE excitation exhibits only the most intense component, as shown in Fig. 6, giving an accurate value of the mode frequency at 1496 cm^{-1}.

As previously mentioned, the narrowness of bands and thus the site-selectivity are absent from the excitation spectra in the S_2 state, even in SE excitation spectra. It is especially observed in H_2TAP doped matrices. The same excitation bands are detected whatever SE band is monitored in Ar and in N_2 (see Fig. 4c and 5d). In N_2, the excitation spectrum seems simplified monitoring SE at 665.6 nm, but the broad band observed is not really characteristic of the probed site. There are at least four effects which can broaden the S_2 bands in the reported excitation spectra: (i) efficient coupling with various vibrational levels of S_1, (ii) the short lifetime of this state, due in part to the previous coupling, (iii) the different S_2–S_1 energy gaps inside a family of sites, which can induce different S_2–S_0 transition energies for different sites whereas the S_1–S_0 transition energies are the same, and (iv) the reabsorption of photons from the S_1–S_0 origin of "blue sites" by "red sites" *via* the excitation of phonons. In the particular case of H_2TAP, (i) and (iv) can be especially important: (i) with a S_2–S_1 splitting of $\sim$2400–2500 cm^{-1}, the S_2 origin lies at the same energy as a dense manifold of S_1 vibrational levels, and (iv) because of the strong electron–phonon coupling observed.

The excitation spectra in the S_2 state of H_2TBP and H_2Pc exhibit different behaviour. For H_2TBP, the S_2–S_1 splitting is $\sim$1800–1900 cm^{-1} and (i) is still important. However, (iv) is not observed in Ar matrices[28] and the excitation spectra of the two close well-resolved SE bands show the same broad and structured bands, but shifted from 4 cm^{-1}, *i.e.* the same shift as in the S_1 state. In this case, the two SE configurations, assigned to the two NH tautomers in the same lattice site,[28] explore the same matrix effect in both the excited states with weak electron–phonon couplings. The S_2–S_1 splitting of H_2Pc is much smaller ($\sim$1000 cm^{-1}), and the S_2 origin is resonant with only few S_1 vibrational levels. Excitation spectra of the SE bands exhibit narrower (and fewer) bands than fluorescence excitation, as shown in Fig. 11 in Ne matrices, which can be explained by a reduced number of sites inside a family of sites defined through the SE process, in comparison with that defined through the fluorescence process, and by the threshold effect. SE may help in the analysis of the S_2–S_1 coupling in this case.

V. Conclusions

We have established that tetrapyrrolic molecules isolated in cryogenic matrices are good systems to obtain stimulated emission in thin samples. Producing emission in the 650–800 nm domain, the exact wavelengths depending on the molecule and on the host, these molecules may thus provide efficient light converters from visible to the deep red range. To the best of our knowledge, no such remarkable SE bands – with large intensities easily detected – were ever observed in matrices with other types of organic molecules and it should be interesting to investigate the behaviour of other dye molecules trapped in cryogenic solids.

Various parameters have been examined to improve the efficiency of SE. Tetrapyrrolic molecules have suitable intrinsic properties to get SE, due to their properties as dyes. SE occurs on a vibronic transition from the vibrationless level of the first excited state (S_1) to specific vibrational levels of the ground state. The most intense vibronic transitions in fluorescence (involving high energy vibrational levels) are good candidates for SE because of their relatively good fluorescence yield and their long wavelengths (*cf.* eqn (1)). H_2TAP was an especially interesting molecule to probe the sensitivity of the mode involved in SE. We showed that two modes at around 1500–1600 cm^{-1} can exhibit SE, with a clear site and host dependence. Only one of them is involved in a given type of environment. This effect results from the influence of phonons in the solid state, which perturbs the intensity distribution of the fluorescence and possibly the vibrational dynamics in the ground state. The mode described by an asymmetric stretch of the bridging C–N–C (or C–C–C in H_2TBP) bonds in the central ring (Fig. 8 and 1) seems to be a preferential one in the stimulated emission behaviour we have explored. A study of vibrational dynamics could help to probe the specificity of this mode.

‡ In ref. 41, the excitation spectrum of the red site in Ne reported in Fig. 9 corresponds erroneously to the excitation of the SE band and not to the excitation of the 0–0 fluorescence band as indicated in the caption.

The fluorescence spectrum of H_2TAP does not show one clearly more intense vibronic band, except the 0–0 one. It explains why SE was observed in a quite numerous amount of transitions, upon high power of the pumping laser, in contrast to the two other molecules. Nevertheless, the transitions of lower frequency in fluorescence remain preferably involved in the SE process. Another peculiarity in the case of H_2TAP relates to the influence of phonons on SE: because of the intense red phonon wings in the fluorescence spectra, SE can be induced by the amplification of spontaneous emission on a vibronic transition of slightly higher energy than the one where SE occurs, as observed in Ar and N_2.

SE was observed in H_2TAP doped matrices despite quite broad vibronic bands arising from strong electron–phonon coupling in the S_1–S_0 transition and the multiplicity of sites. Without any quantitative measurement, it seems that SE was however more easily observed in samples exhibiting a limited number of "well-defined" trapping sites and where the electron–phonon coupling was weaker. In the latter case, the density of emitting centers at the SE wavelength is higher, which helps to induce SE. We have checked this effect with the phthalocyanine family: it was easier to observe SE with the free-base (H_2Pc) and ZnPc than with AlPc and the explanation may be the non-planarity of AlPc, which is more difficult to trap in crystallographic planes, and thus explores more different environments. SE was also more efficient in systems without heavy atoms. The heavy atom effect enhances the intersystem crossing towards the molecular triplet state after the laser excitation. The S_1 state lifetime is then too short compared to the laser pulse duration so that accumulation of excited molecules within the temporal width of excitation pulse is difficult and the density of fluorescence photons is too weak for SE to occur. Nevertheless, despite its short lifetime, SE was detected with H_2TAP in the three studied hosts.

Following the previous discussion, tetrapyrrolic molecules embedded in Shpol'skii matrices appear to be ideal hosts to achieve SE easily. Electronic spectra of H_2Pc,[50] H_2TBP,[51] H_2TAP[52] in Shpol'skii matrices at low temperature exhibit very narrow lines. Emission and excitation spectra show vibronic transitions as doublets corresponding to the two NH tautomers and these solids are especially suitable to document the NH tautomerism process.[53] We have tried to use such media for SE experiments, but our attempts were unsuccessful because the density of trapped molecules in the samples was too low, due to the low solubility of the tetrapyrrolic species. Other attempts and the search for other suitable environments are still in progress.

Acknowledgements

This work was supported by the BRFFR-CNRS exchange grants (F09F-001/23181 and F11F-001/24 692) and the CNRS projects. The assistance of the Ulysses France-Ireland research exchange grant (2011) is also acknowledged as are Tatiana Pavich for the synthesis of H_2TAP and Chris Henchy for providing DFT results and for his help in the preparation of Fig. 8.

References

1 G. Bottari, O. Trukhina, M. Ince and T. Torres, *Coord. Chem. Rev.*, 2012, **256**, 2453–2477.
2 C. K. C. Bikram, N. K. Subbaiyan and F. D'Souza, *J. Phys. Chem. C*, 2012, **116**, 11964–11972.
3 S. Mathew, A. Yella, P. Gao, R. Humphry-Baker, B. F. E. Curchod, N. Ashari-Astani, I. Tavernelli, U. Rothlisberger, M. K. Nazeeruddin and M. Grätzel, *Nat. Chem.*, 2014, **6**, 242–247.
4 A. Yella, H.-W. Lee, H. N. Tsao, C. Yi, A. K. Chandiran, M. K. Nazeeruddin, E. W.-G. Diau, C.-Y. Yeh, S. M. Zakeeruddin and M. Grätzel, *Science*, 2011, **334**, 629–634.
5 S. Karthikeyan and J. Y. Lee, *J. Phys. Chem. A*, 2013, **117**, 10973–10979.
6 L.-L. Li and E. W.-G. Diau, *Chem. Soc. Rev.*, 2013, 291–304.
7 K. Ogawa and Y. Kobuke, in *Nonlinear Optics*, ed. N. Kamanina, InTech, 2012, pp. 209–224.
8 K. Ogawa and Y. Kobuke, *Org. Biomol. Chem.*, 2009, **7**, 2241–2246.
9 Y. Amao and I. Okura, *J. Porphyrins Phthalocyanines*, 2009, **13**, 1111–1122.
10 İ. Capan, Ç. Tarımcı and R. Capan, *Sens. Actuators, B*, 2010, **144**, 126–130.
11 D. Mondal and S. Bera, *Adv. Nat. Sci.: Nanosci. Nanotechnol.*, 2014, **5**, 033002.
12 E. D. Sternberg, D. Dolphin and C. Brückner, *Tetrahedron*, 1998, **54**, 4151–4202.
13 Z. J. Wang, B. Chauvin, P. Maillard, F. Hammerer, D. Carez, A. Croisy, C. Sandré, S. Chollet-Martin, P. Prognon, J. L. Paul, J. Blais and A. Kasselouri, *J. Photochem. Photobiol., B*, 2012, **115**, 16–24.
14 Z. Chen, P. Xu, J. Chen, H. Chen, P. Hu, X. Chen, L. Lin, Y. Huang, K. Zheng, S. Zhou, R. Li, S. Chen, J. Liu, J. Xue and M. Huang, *Acta Biomater.*, 2014, **10**, 4257–4268.
15 *Handbook of Porphyrin Science*, World Scientific, http://www.worldscientific.com/worldscibooks/10.1142/8560-vol33#t=aboutBook.
16 A. E. Pullen, C. Faulmann and P. Cassoux, *Eur. J. Inorg. Chem.*, 1999, 269–276.
17 R. F. Linstead and M. Whalley, *J. Chem. Soc.*, 1952, 4839–4846.
18 O. G. Khelevina, N. V Chizhova and P. A. Stuzhin, *J. Porphyrins Phthalocyanines*, 2000, **4**, 555–563.
19 M. Gouterman, *J. Mol. Spectrosc.*, 1961, **6**, 138–163.
20 G. A. Kumar, J. Thomas, N. V. Unnikrishnan, V. P. N. Nampoori and C. P. G. Vallabhan, *J. Porphyrins Phthalocyanines*, 2001, **5**, 456–459.
21 D. Wöhrle, G. Schnurpfeil, S. G. Makarov, A. Kazarin and O. N. Suvorova, *Macroheterocycles*, 2012, **5**, 191–202.
22 P. Gregory, *J. Porphyrins Phthalocyanines*, 2000, **4**, 432–437.
23 B. I. Stepanov, A. N. Rubinov and V. A. Mostovnikov, *JETP Lett.*, 1967, **5**, 117–119.
24 P. P. Sorokin, J. R. Lankard, E. C. Hammond and V. L. Moruzzi, *IBM J. Res. Dev.*, 1967, **11**, 130.
25 P. P. Sorokin and J. R. Lankard, *IBM J. Res. Dev.*, 1966, **10**, 162.

26 N. Dozova, C. Murray, J. G. McCaffrey, N. Shafizadeh and C. Crépin, *Phys. Chem. Chem. Phys.*, 2008, **10**, 2167–2174.
27 R. Pellow and M. Vala, *J. Chem. Phys.*, 1989, **90**, 5612.
28 C. Crépin, N. Shafizadeh, W. Chin, J. P. Galaup, J. G. McCaffrey and S. M. Arabei, *Low Temp. Phys.*, 2010, **36**, 451–457.
29 S. M. Arabei, J. P. Galaup, J. G. McCaffrey, N. Shafizadeh and C. Crépin, *Low Temp. Phys.*, 2012, **38**, 727–731.
30 D. R. Tackley, G. Dent and W. E. Smith, *Phys. Chem. Chem. Phys.*, 2001, **3**, 1419–1426.
31 C. Murray, N. Dozova, J. G. McCaffrey, S. FitzGerald, N. Shafizadeh and C. Crépin, *Phys. Chem. Chem. Phys.*, 2010, **12**, 10406–10422.
32 S. F. Shkirman, L. L. Gladkov, V. K. Konstantinova and K. N. Solovyov, *Spectrosc. Lett.*, 1998, **31**, 1749–1760.
33 C. Henchy, J. G. McCaffrey, S. Arabei, T. Pavich, J.-P. Galaup, N. Shafizadeh and C. Crépin, *J. Chem. Phys.*, 2014, **141**, 124303.
34 J. G. Radziszewski, J. Waluk and J. Michl, *J. Mol. Spectrosc.*, 1990, **140**, 373–389.
35 J. G. Radziszewski, J. Waluk, M. Nepras and J. Michl, *J. Phys. Chem.*, 1991, **95**, 1963–1969.
36 S. S. Dvornikov, V. N. Knyukshto, V. A. Kuzmitsky, A. M. Shulga and K. N. Solovyov, *J. Lumin.*, 1981, **23**, 373–392.
37 E. A. Makarova, G. V Korolyova, O. L. Tok and E. A. Lukyanets, *J. Porphyrins Phthalocyanines*, 2000, **4**, 525–531.
38 S. M. Arabei, V. A. Kuzmitsky and K. N. Solovyov, *Opt. Spectrosc.*, 2007, **102**, 692–704.
39 G. I. Peters and L. Allen, *J. Phys. A: Gen. Phys.*, 1971, **4**, 238–243.
40 L. Allen and G. I. Peters, *Phys. Rev. A: At., Mol., Opt. Phys.*, 1973, **8**, 2031–2047.
41 C. Murray, N. Dozova, J. G. McCaffrey, N. Shafizadeh, W. Chin, M. Broquier and C. Crépin, *Phys. Chem. Chem. Phys.*, 2011, **13**, 17543–17554.
42 C. A. Murray, *PhD thesis*, National University of Ireland Maynooth, 2010.
43 A. T. Gradyushko, A. N. Sevchenko, K. N. Solovyov and M. P. Tsvirko, *Photochem. Photobiol.*, 1970, **11**, 387–400.
44 P. P. Pershukevich, D. I. Volkovich, L. L. Gladkov, S. V. Dudkin, A. P. Stupak, V. A. Kuzmitsky, E. A. Makarova and K. N. Solovyov, *Opt. Spectrosc.*, 2014, **117**, 722–740.
45 D. S. Lawrence and D. G. Whitten, *Photochem. Photobiol.*, 1996, **64**, 923–935.
46 P. S. Vincett, E. M. Voigt and K. E. Rieckhoff, *J. Chem. Phys.*, 1971, **55**, 4131.
47 V. A. Kuz'mitskii, K. N. Solov'ev, V. N. Knyukshto, I. K. Shushkevich, V. N. Kopranenkov and A. M. Vorotnikov, *Theor. Exp. Chem.*, 1983, **19**, 604–611.
48 K. N. Solovyov, L. L. Gladkov, A. S. Starukhin and S. F. Shkirman, *Porphyrine Spectroscopy: Vibrational States*, Nauka i Tekhnika, Minsk, 1985, pp. 191–198.
49 A. Kyrychenko and J. Waluk, *J. Chem. Phys.*, 2003, **119**, 7318.
50 T. H. Huang, K. E. Rieckhoff and E. M. Voigt, *J. Chem. Phys.*, 1982, **77**, 3424–3441.
51 S. M. Arabei, K. N. Solov'ev and Y. I. Tatulchenkov, *Opt. Spektrosk.*, 1992, **73**, 686–693.
52 W. Y. Huang, S. Salmon, G. JeanCharles, E. VanRiper and L. W. Johnson, *Spectrochim. Acta, Part A*, 1996, **52**, 157–166.
53 K. N. Solov'ev, I. E. Zalesskii, V. N. Kotlo and S. F. Shkirman, *JETP Lett.*, 1973, **17**, 332.

